Hindawi
Journal of Chemistry
Volume 2019, Article ID 2505823, 10 pages
https://doi.org/10.1155/2019/2505823

Research Article

Oxidative Degradation of Amoxicillin in Aqueous Solution by Thermally Activated Persulfate

Juanjuan Zhao,[1,2] Yujiao Sun,[1] Fachao Wu,[2] Minjian Shi,[2] and Xurui Liu[2]

[1]*College of Water Sciences, Beijing Normal University, Beijing 100875, China*
[2]*Environmental Engineering Department, North China Institute of Science and Technology, Beijing 101601, China*

Correspondence should be addressed to Yujiao Sun; sun201405@163.com

Received 27 September 2018; Revised 10 February 2019; Accepted 17 February 2019; Published 12 March 2019

Guest Editor: Giuseppe Meca

Antibiotic residues and antibiotic resistance genes (ARGs) pose a great threat to public health and food security via the horizontal transfer in the food production chain. Oxidative degradation of amoxicillin (AMO) in aqueous solution by thermally activated persulfate (TAP) was investigated. The AMO degradation followed a pseudo-first-order kinetic model at all tested conditions. The pseudo-first-order rate constants of AMO degradation well-fitted the Arrhenius equation when the reaction temperature ranged from 35°C to 60°C, with the apparent activate energy of 126.9 kJ·mol^{-1}. High reaction temperature, high initial persulfate concentration, low pH, high Cl^- concentration, and humic acid (HA) concentration increased the AMO degradation efficiency. The EPR test demonstrated that both ·OH and $SO_4^{\cdot-}$ were generated in the TAP system, and the radical scavenging test identified that the predominant reactive radical species were $SO_4^{\cdot-}$ in aqueous solution without adjusting the solution pH. In groundwater and drinking water, AMO degradation suggested that TAP could be a reliable technology for water remediation contaminated by AMO in practice.

1. Introduction

Antibiotic residues ubiquitously exist in surface water, groundwater, and soil because of overuse and misuse in human and veterinary medicines, leading to the prevalence of antibiotic resistance genes (ARGs) in natural environment [1]. ARGs as a kind of emerging contaminants pose a great threat to public health and food security mainly due to the persistence in environment and the horizontal transfer in the food production chain [2, 3]. Thus, it is urgent to take effective measures to eliminate the antibiotics in natural environment in order to reduce the influence of ARGs.

Advanced oxidation processes (AOPs) which could produce highly active, oxidizing radicals such as hydroxyl radicals, sulfate radicals, and other radicals are promising techniques to degrade recalcitrant contaminants into harmless products (CO_2 and H_2O) [4–6]. Recently, sulfate radical-based AOPs has received increasing amount of interest due to its low cost, high efficiency, and friendly environment in degradation and mineralization of recalcitrant contaminants [7]. Persulfate (PS) is usually applied as the precursor of sulfate radicals by reaction equation (1):

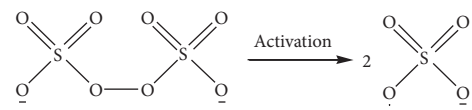

(1)

Sulfate radicals could be generated through scission of the peroxide bond of persulfate by energy including heat [8, 9], ultraviolet [5, 10], ultrasound [11], radiolysis [12], and catalyzer [13–16]. Among these methods, TAP is particularly attractive for removing organic contaminants because it is a simple and effective method to produce sulfate radicals with a high reaction stoichiometric efficiency (RSE) [17]. In this study, amoxicillin (AMO) belonging to β-lactam antibiotic, which was the top-priority human and veterinary antibiotic, was chosen as the target contaminant. Currently, AMO was degraded by various physical-chemical processes including the use of zero-valent iron [18, 19] and AOPs such as Fenton's reagent [20, 21], photo-Fenton process [22, 23], UV

and UV/H_2O_2 processes [24], microwave-assisted Fenton's oxidation [25], photocatalytic adsorbents [26], photocatalytic ozonation process [27], and photo-Fenton process with Goethite [28]. To the best of our knowledge, this is the first report on oxidative degradation of AMO by TAP in aqueous solution.

The aim of this present study was to investigate TAP for the remediation of highly AMO-contaminated water, including the influence factors of the reaction temperature, initial PS concentration, pH and Cl^-, Ca^{2+}, Mg^{2+}, humic acid (HA), and dissolved oxygen. The predominant radicals were identified by electron paramagnetic resonance (EPR), and AMO degradation in real waters was evaluated, which provides fundamental and practical knowledge to treat AMO-contaminated waters.

2. Materials and Methods

2.1. Chemicals and Materials. Amoxicillin trihydrate ($C_{16}H_{19}N_3O_5S{\cdot}3H_2O$, AMO, ≥98.0%), humic acid (FA ≥ 90%), and *tert*-butyl alcohol ($(CH_3)_3COH$, TBA, ≥99.5%) were obtained from Aladdin Industrial Corporation (Shanghai, China). Sodium persulfate ($Na_2S_2O_8$, PS, ≥98%) was purchased from Thermo Fisher Scientific (New Jersey, USA). Methanol (CH_3OH, MeOH, HPLC grade) was obtained from J. T. Baker (USA). 5,5-Dimethyl-1-pyrrolidine-N-oxide (DMPO) was acquired from Macklin Biochemical Co. Ltd (Shanghai, China).

2.2. Water Samples. Groundwater was collected from a well in Nanxin village (40°3′32.9″N, 116°47′50.9″E) (Beijing, China), and drinking water was taken from Yanjiao town (39°57′18.3″N, 116°48′11.6″E) (Hebei, China). All the water samples were filtered through a 0.22 μm membrane and stored at 4°C before further experiments.

2.3. Experimental Procedures. All experiments were performed in 250 mL conical flasks with ground glass stoppers. At the beginning of every experiment, a 10.00 mL·1.010 mmol·L^{-1} AMO stock solution was diluted to 100.00 mL and heated to the designated temperature for 20 min. The reaction was started by the addition of 1.00 mL·1.010 mol·L^{-1} PS stock solution; therefore, $[AMO]_0$ was 0.1 mM, and $[PS]_0$ was 10 mM. 1.00 mL samples were removed from the conical flask at each desired time interval and quickly quenched by 1.00 mL methanol before analysis. The initial pH values of the solution were adjusted by 1.0 mol·L^{-1} NaOH and H_2SO_4 in order to investigate the effects of the initial pH. TBA and MeOH as scavenging agents were applied to identify the dominating radicals in the TAP system. All the samples were performed in triplicates, and the standard deviations were depicted as error bars in figures. The control experiments were performed without PS at the same conditions.

2.4. Analytical Methods. The concentration of AMO was analyzed using a high pressure liquid chromatography (LC-20AT, Shimadzu, Japan) equipped with a WondaSil C18-WR column (5 μm, 4.6 mm × 250 mm, GL Sciences Inc., Japan). The mobile phase was made of a mixture of 80% ultrapure water and 20% methanol, and the flow rate was 1.0 mL/min. The column temperature was maintained at 40°C. 10 μL of sample was injected into the HPLC. A FiveEasy plus pH meter (Mettler Toledo) was applied to test the solution pH. A MS-5000 electron paramagnetic resonance (EPR) instrument (Freiberg instruments, Germany) was applied to identify radical species in the TAP system under the following instrument conditions: modulation amplitude, 1.0 G; modulation frequency, 100 kHz; sweep width, 100 G; sweep time, 120 s; and microwave power, 10.00 mW. Cl^-, NO_3^-, and SO_4^{2-} were analyzed by the ICS-2100 ion chromatograph (Dionex, USA) with Ionpac AS11 column, and Na^+, NH_4^+, K^+, Mg^{2+}, and Ca^{2+} were analyzed by the AQ ion chromatograph (Thermo Fisher, USA) using the Ionpac CS12A column. PS concentration was monitored according to previous literature [29]. Total organic carbon (TOC) was measured by a vario TOC analyzer (Elementar, Germany).

3. Results and Discussion

3.1. Effects of Reaction Temperature on Degradation of AMO. Reaction temperature is a critical factor that should be considered for applying TAP to degrade organic contaminants. Effects of the reaction temperature (35–60°C) on AMO degradation by TAP are shown in Figure 1(a). It could be seen that AMO oxidative degradation was temperature dependent. There was only 22% AMO oxidized by persulfate at 35°C within 330 min. However, obvious degradation was observed with the increasing temperature. The removal of AMO was completely achieved by TAP at 55°C within 330 min, and the complete degradation time was decreased to 90 min at 60°C.

In addition, the AMO degradation well-fitted a pseudo-first-order kinetic model as shown in the following equation:

$$-\frac{dC}{dt} = k_{obs}C. \tag{2}$$

It can also be written as follows:

$$\ln\frac{C}{C_0} = -k_{obs}t. \tag{3}$$

k_{obs} was the pseudo-first-order rate constants (min^{-1}), and it was determined by the plots of $\ln(C/C_0)$ versus reaction time (t), as shown in Figure 1(b). $t_{1/2}$ was defined as equation (4), and kinetic parameters of AMO degradation by TAP at different conditions are shown in Table 1:

$$t_{1/2} = \frac{\ln 2}{k_{obs}} = \frac{0.6931}{k_{obs}}, \tag{4}$$

$$\ln k_{obs} = \ln A - \frac{E_a}{RT}, \tag{5}$$

$$\ln k_{obs} = 42.21 - \frac{15267.38}{T}. \tag{6}$$

k_{obs} in the oxidative degradation by TAP increased significantly when the reaction temperature raised from

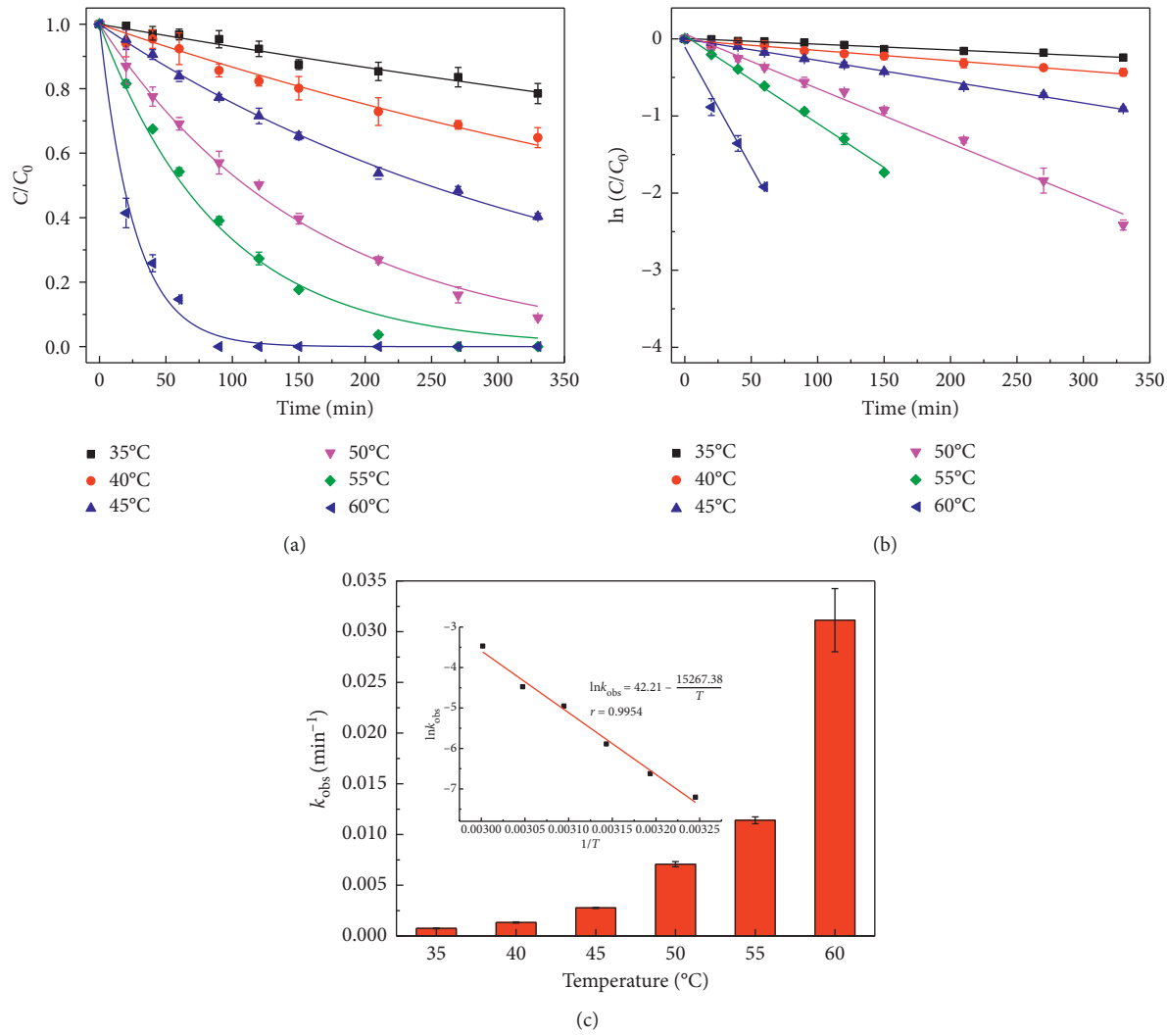

FIGURE 1: Effects of reaction temperature on AMO degradation by TAP (a). Plot of $\ln(C/C_0)$ versus reaction time t for k_{obs} determination with the pseudo-first-order kinetic model (b). Plot of $\ln k_{obs}$ versus $1/T$ for E_a determination with the Arrhenius equation (c). Experimental conditions: $[AMO]_0 = 0.1$ mM; $[PS]_0 = 10$ mM; $T = 35$–60°C; reaction time = 330 min.

35°C to 60°C. Furthermore, $\ln k_{obs}$ and $1/T$ followed Arrhenius equation (5), and AMO degradation by TAP was identified as equation (6) with high correlation coefficient ($r = 0.9942$). The apparent activate energy (E_a) of AMO degradation was calculated to be 126.9 kJ·mol^{-1} according to equation (6), which was comparable to those of other refractory organics, such as ketoprofen (157.02(±8.9) kJ·mol^{-1}) [10], triclosan (121 kJ·mol^{-1}) [30], naproxen (155 kJ·mol^{-1}) [31], ibuprofen (168(±9.5) kJ·mol^{-1}) [9], bisoprolol (119.8(±10.8) kJ·mol^{-1}) [17], and diuron (166.7 kJ·mol^{-1}) [32]. These comparable apparent activate energy indicated that the TAP system could be suitable for degrading refractory organics in wastewater treatment.

3.2. Effects of Initial PS Concentration on Degradation of AMO. PS concentration is also a significant factor that influences AMO degradation by TAP. Effects of $[PS]_0$ on AMO degradation are shown in Figure 2. AMO degradation followed the pseudo-first-order kinetic model, and AMO degradation efficiency increased with increasing $[PS]_0$ from 2 to 20 mM. There was about 31, 54, 91, and 100% AMO degraded at 330 min in the TAP system when $[PS]_0$ was 2, 5, 10, and 15 mM, respectively. All of AMO was removed at 20 mM $[PS]_0$ at 210 min. Furthermore, k_{obs} increased linearly with increasing $[PS]_0$ according to Figure 2(c), suggesting that the AMO degradation rate was in positively proportion to $[PS]_0$. Similar phenomenon observed by Yang et al. [33], Chen et al. [34], and Nie et al. [35] was possibly due to more $SO_4^{\cdot-}$ released by high concentration of TAP.

% RSE defined as the ratio of the concentration of the polluters degraded to the PS consumed [15, 31] is a critical parameter to evaluate the sustainability of TAP. % RSE values at different $[PS]_0$ values in the TAP system at reaction time of 330 min are shown in Figure 3. The maximum % RSE value was reached at $[PS]_0 = 10$ mM. When $[PS]_0$ increased from 2 mM to 10 mM, % RSE increased gradually with the increase of AMO degradation efficiency. When $[PS]_0$ was from 10 mM to 20 mM, % RSE decreased due to the quenching reactions between radical and radical or radical

Table 1: Kinetic parameters of AMO degradation by TAP at different conditions.

Operating conditions	k_{obs} (min^{-1})	$t_{1/2}$ (min)	r
$[AMO]_0 = 0.1$ mM, $[PS]_0 = 10$ mM			
$T = 35^{\circ}C$	0.0007	990.14	0.9886
$T = 40^{\circ}C$	0.0013	533.15	0.9924
$T = 45^{\circ}C$	0.0028	247.54	0.9985
$T = 50^{\circ}C$	0.0071	97.62	0.9949
$T = 55^{\circ}C$	0.0114	60.80	0.9978
$T = 60^{\circ}C$	0.0311	22.29	0.9902
$[AMO]_0 = 0.1$ mM, $T = 50^{\circ}C$			
$[PS]_0 = 2$ mM	0.0013	533.15	0.9894
$[PS]_0 = 5$ mM	0.0024	288.79	0.9894
$[PS]_0 = 10$ mM	0.0071	97.62	0.9949
$[PS]_0 = 15$ mM	0.0092	75.34	0.9959
$[PS]_0 = 20$ mM	0.0165	42.01	0.9965
$[AMO]_0 = 0.1$ mM, $[PS]_0 = 10$ mM, $T = 50^{\circ}C$			
pH = 2	0.0159	43.59	0.9992
pH = 5	0.0067	103.45	0.9738
pH = 8	0.0060	115.52	0.9920
pH = 10	0.0058	119.50	0.9991
$[Cl^-]_0 = 1$ mM	0.0058	119.50	0.9968
$[Cl^-]_0 = 10$ mM	0.0082	84.52	0.9825
$[Cl^-]_0 = 100$ mM	0.0082	84.52	0.9944
$[HA]_0 = 0.1$ mg/L	0.0097	71.31	0.9752
$[HA]_0 = 1$ mg/L	0.0103	67.16	0.9768
$[HA]_0 = 10$ mg/L	0.0103	67.10	0.9836
$[HA]_0 = 20$ mg/L	0.0098	70.72	0.9727
$[Ca^{2+}]_0 = 1$ mM	0.0073	94.95	0.9978
$[Mg^{2+}]_0 = 1$ mM	0.0074	93.66	0.9948
Groundwater	0.0059	117.47	0.9920
Drinking water	0.0053	130.77	0.9968

and PS [5]. The TOC removal increased with the increasing $[PS]_0$ from 2 mM to 20 mM, as depicted in Figure 3. This phenomenon might be due to the attacking on AMO and its degradation intermediates by the radicals formed at high PS concentrations. It can be clearly seen that high TOC removal and high % RSE were not reached at the same time in Figure 3. This was in accordance with the literature reported by Ghauch et al. [5].

3.3. Effects of Solution pH on Degradation of AMO. Solution pH is an important factor for TAP to degrade contaminants because it could obviously affect radical species, contaminant formations, and reaction mechanisms. Effects of different pH values on AMO degradation by TAP are shown in Figure 4. As it can be seen, AMO degradation efficiency increased significantly with decreasing pH, indicating that lower pH was favorable to degrade AMO. This result was consistent with the previous reports about sulfate radical-based oxidation of fluoroquinolone [36] and triclosan [30]. This phenomenon could be explained as follows.

(i) The predominant radical species were affected by solution pH. At acid conditions, sulfate radical was the dominating radicals, formed as equations (7) and (8), and the reactivity increased with decreasing pH. At basic conditions, hydroxyl radical was the main radical converted from sulfate radical by using equation (9):

$$S_2O_8^{2-} + H^+ \longrightarrow HS_2O_8^- \quad (7)$$

$$HS_2O_8^- \longrightarrow SO_4^{\cdot-} + HSO_4^{\cdot} \quad (8)$$

$$SO_4^{\cdot-} + OH^- \longrightarrow {\cdot}OH + SO_4^{2-} \quad (9)$$

Therefore, the reaction mechanisms with contaminants would vary with the predominant radicals. It is reported that $SO_4^{\cdot-}$ reacts with recalcitrant compounds by electron transfer [37], addition-elimination, and hydrogen atom abstraction [38], while ·OH reacts with recalcitrant compounds by addition of C=C double bonds or abstraction of hydrogen from the C-H, N-H, or O-H bond [39].

(ii) AMO speciation changed with the changing of solution pH, as shown in Figure 5. When $pH < pK_{a1}$ of AMO (2.4), an AMO molecule accepts a proton forming an ion with a positive charge. When pK_{a1} (2.4) $< pH < pK_{a2}$ (7.4), AMO exists in the form of molecule in aqueous solution. When pK_{a2} (7.4) $< pH < pK_{a3}$ (9.6), an AMO molecule loses a proton forming an ion with a negative charge. When $pH > pK_{a3}$ (9.6), an AMO molecule loses two protons forming an ion with two negative charges. As shown in Figure 4, the highest k_{obs} was attained at pH 2 due to the protonation of AMO, resulting in AMO^+ with a positive charge which increased the electrostatic attraction to $SO_4^{\cdot-}$. With the increase in pH, k_{obs} decreased which could also be attributed by the deprotonation of AMO, resulting in the electrostatic repulsion to $SO_4^{\cdot-}$.

3.4. Effects of Matrix in Aqueous Solution on Degradation of AMO

3.4.1. Cl^- Concentration. The effects of different anions on AMO degradation were studied. Figure 6 shows the effects of Cl^- concentration. When Cl^- concentration was 1 mM, k_{obs} was slightly lower than that in deionized water, and when Cl^- concentration was 10 mM and 100 mM, k_{obs} was a little higher, indicating that higher Cl^- concentration could promote AMO oxidative degradation. This phenomenon was identical with the effect of Cl^- concentration on the degradation of sulfamethazine by TAP [40]. It was probably due to the formation of reactive chlorine species including $Cl^{\cdot}$, $Cl_2^{\cdot-}$, Cl_2, and HOCl, which were moderate oxidants produced by reactions (10)–(13) [41] and could react with AMO molecular to promote AMO degradation efficiency:

$$SO_4^{\cdot-} + Cl^- \longrightarrow SO_4^{2-} + Cl^{\cdot}, \quad E^0\left(\frac{Cl^{\cdot}}{Cl^-}\right) = 2.41 \text{ V} \quad (10)$$

$$Cl^{\cdot} + Cl^- \longrightarrow Cl_2^{\cdot-}, \quad E^0\left(\frac{Cl_2^{\cdot-}}{Cl^-}\right) = 2.09 \text{ V} \quad (11)$$

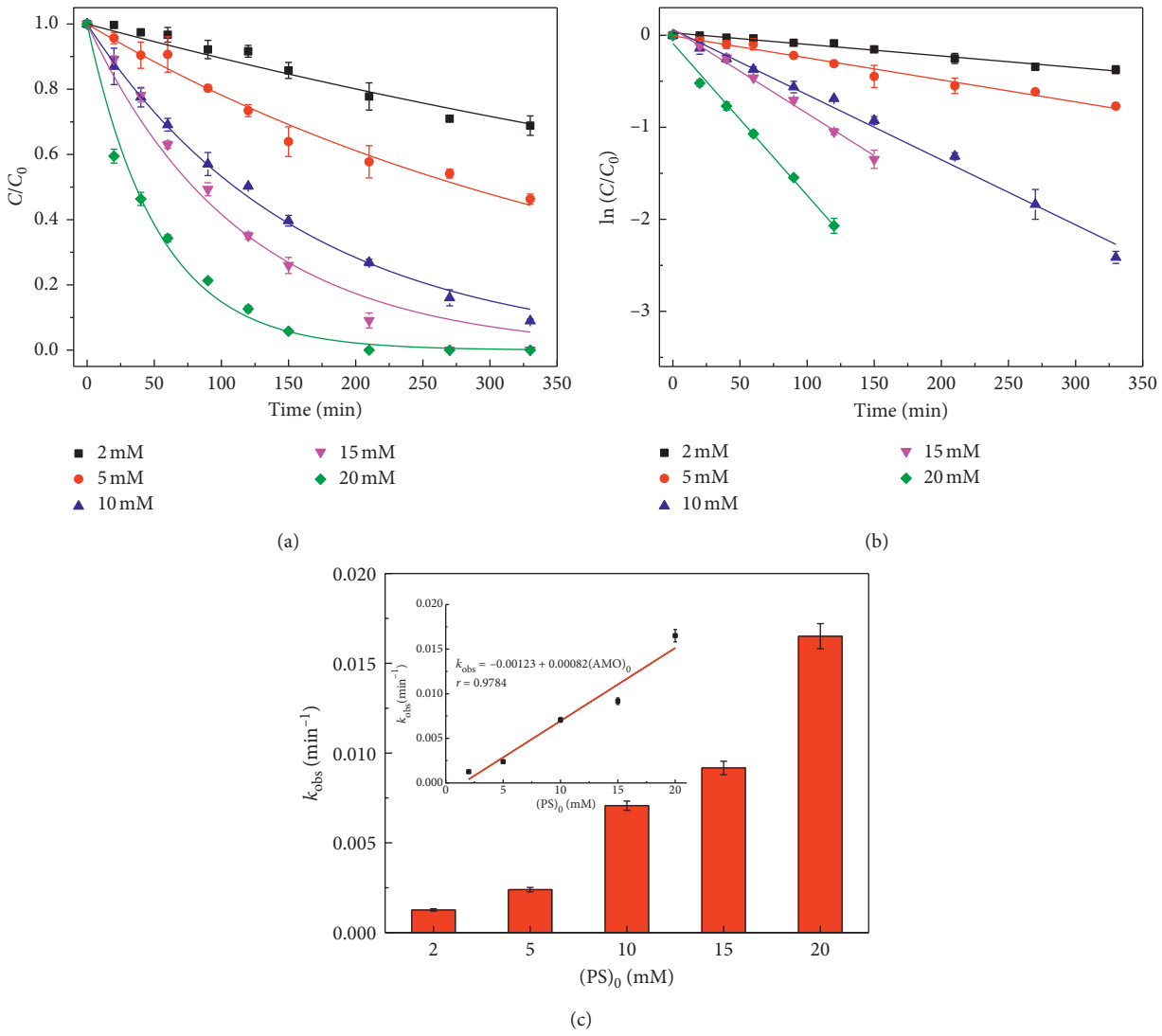

FIGURE 2: Effects of $[PS]_0$ on AMO degradation by TAP (a). Plot of $\ln(C/C_0)$ versus reaction time t for k_{obs} determination with the pseudo-first-order kinetic model (b). Plot of k_{obs} versus $[PS]_0$ (c). Experimental conditions: $[AMO]_0 = 0.1$ mM; $[PS]_0 = 2$–20 mM; $T = 50^{\circ}$C; reaction time = 330 min.

$$Cl_2^{\cdot-} + Cl_2^{\cdot-} \longrightarrow 2Cl^- + Cl_2, \quad E^0\left(\frac{Cl_2}{Cl^-}\right) = 1.36 \text{ V} \tag{12}$$

$$Cl_2 + H_2O \longrightarrow HOCl + Cl^- + H^+, \quad E^0\left(\frac{HOCl}{Cl^-}\right) = 1.48 \text{ V} \tag{13}$$

3.4.2. Ca^{2+} and Mg^{2+}. Ca^{2+} and Mg^{2+} are common cations in aqueous matrices which contribute to the water hardness. Effects of Ca^{2+} and Mg^{2+} on AMO degradation by TAP are shown in Figure 7. % change in k_{obs} of Ca^{2+} and Mg^{2+} in aqueous solution defined as equation (14) was 2.82% and 4.22%, respectively, which indicated that Ca^{2+} and Mg^{2+} had no effect on AMO degradation. This result was consistent with the effects of Ca^{2+} and Mg^{2+} on ketoprofen degradation because Ca^{2+} and Mg^{2+} could not activate persulfate [42]:

$$\% \text{ change in } k_{obs} = \frac{(k_{obs}, \text{with cation} - k_{obs}, \text{deionized water})}{k_{obs}, \text{deionized water}} \times 100\%. \tag{14}$$

3.4.3. HA Concentration. Humic acid (HA) is naturally abundant in groundwater, river water, soils, and sediments, and understanding the effects of HA on the degradation of organic compounds is important to apply TAP to *in situ* chemical remediation (ISCO). The effects of HA on AMO degradation are investigated and shown in Figure 8. AMO degradation efficiency increased gradually with the increase of HA concentration from 0.1 to 10 mg/L, indicating that HA

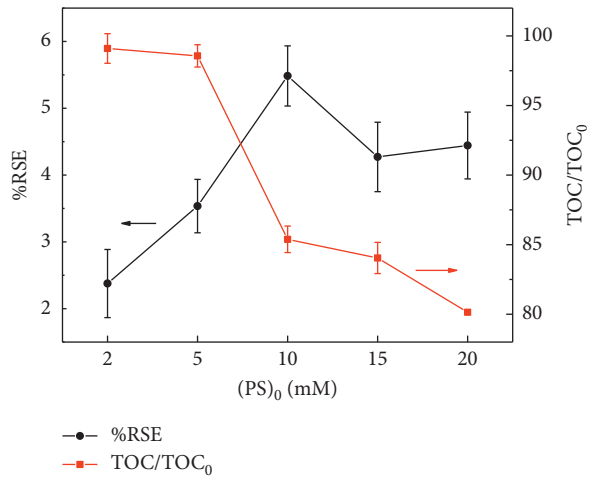

Figure 3: % RSE and TOC/TOC_0 at different $[PS]_0$ in the TAP system. Experimental conditions: $[AMO]_0 = 0.1$ mM; $[PS]_0 = 2$–20 mM; $T = 50^{\circ}C$; reaction time = 330 min.

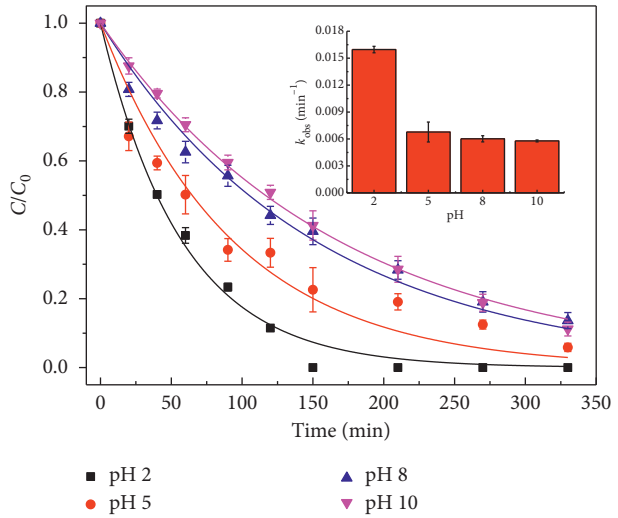

Figure 4: Effects of pH on AMO degradation by TAP. Solid lines represent the pseudo-first-order kinetic model fits. Insert: changes of k_{obs} at different pH values. Experimental conditions: $[AMO]_0 = 0.1$ mM; $[PS]_0 = 10$ mM; $T = 50^{\circ}C$; reaction time = 330 min.

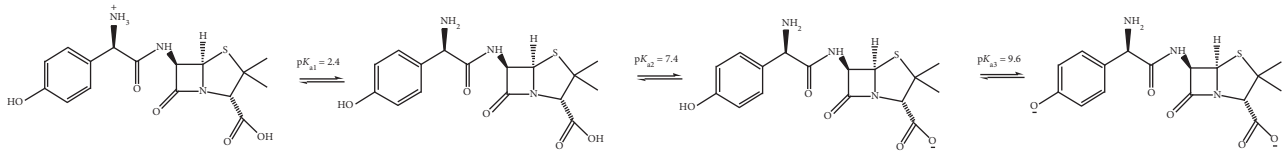

Figure 5: Changes of AMO speciation by solution pH.

could promote AMO degradation efficiency obviously. This phenomenon was consistent with some previous reports. The quinone functional groups in HA could efficiently activate persulfate to degrade 2,4,4′-trichlorobiphenyl was verified, and the activation of persulfate was induced by the formation of semiquinone radicals [43]. Phenol-activated persulfate by the phenoxide form was investigated, and the significant role of phenol in the activation of persulfate was documented by Ahmad [44]. Thus, the increasement on AMO degradation was possibly due to the contribution of quinone and phenol functional groups in HA. When HA concentration continuously increased to 20 mg/L, the AMO degradation efficiency decreased a little compared with that in 1–10 mg/L HA solution possibly due to the HA's quenching effect to $SO_4^{\cdot-}$ and ·OH because of the electron-rich sites in HA [10].

3.4.4. Dissolved Oxygen. In order to investigate the effect of dissolved oxygen on AMO degradation by TAP, three

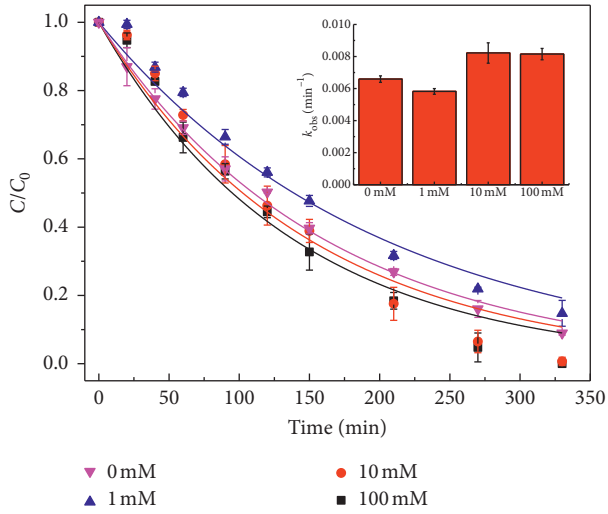

Figure 6: Effects of Cl^- concentration on AMO degradation by TAP. Solid lines represent the pseudo-first-order kinetic model fits. Insert: changes of k_{obs} at different Cl^- concentrations. Experimental conditions: $[AMO]_0 = 0.1$ mM; $[PS]_0 = 10$ mM; $T = 50^\circ$C; reaction time = 330 min.

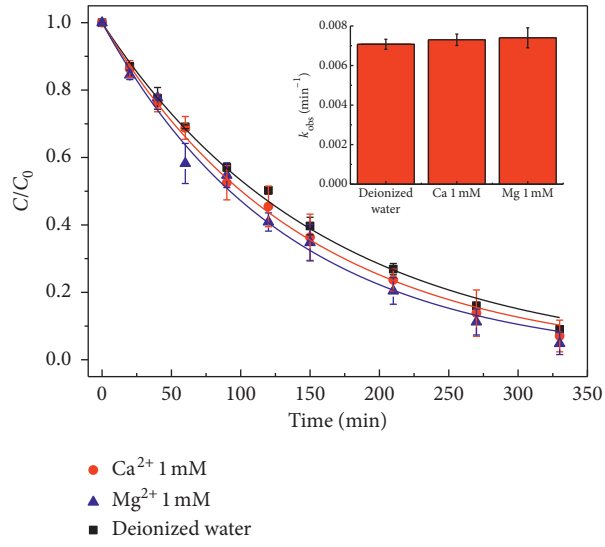

Figure 7: Effects of different cations on AMO degradation by TAP. Solid lines represent the pseudo-first-order kinetic model fits. Insert: changes of k_{obs} at different pH values. Experimental conditions: $[AMO]_0 = 0.1$ mM; $[PS]_0 = 10$ mM; $T = 50^\circ$C; reaction time = 330 min.

systems were designed as follows: System 1 was operated as depicted in Section 2.3 as the control experiment; System 2 was conducted in a closed vial and before reaction nitrogen was filled in order to remove oxygen in solution and conical flask. System 3 was carried out in an open vial. The results are shown in Figure 9. It can be seen that the AMO degradation rate was higher in System 3 than in System 2, suggesting that the oxic condition facilitated the degradation rate of AMO by TAP. However, at reaction time of 330 min, AMO degradation efficiency remained between 88% and 91% under a different dissolve oxygen, demonstrating that the

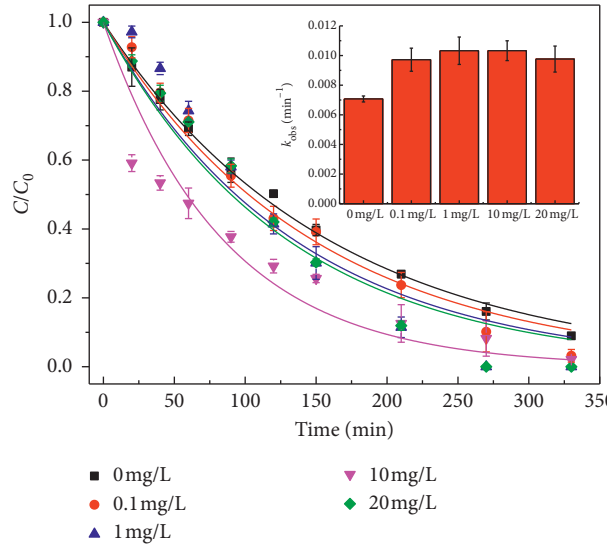

Figure 8: Effects of HA concentration on AMO degradation by TAP. Solid lines represent the pseudo-first-order kinetic model fits. Insert: changes of k_{obs} at different HA concentrations. Experimental conditions: $[AMO]_0 = 0.1$ mM; $[PS]_0 = 10$ mM; $T = 50^\circ$C; reaction time = 330 min.

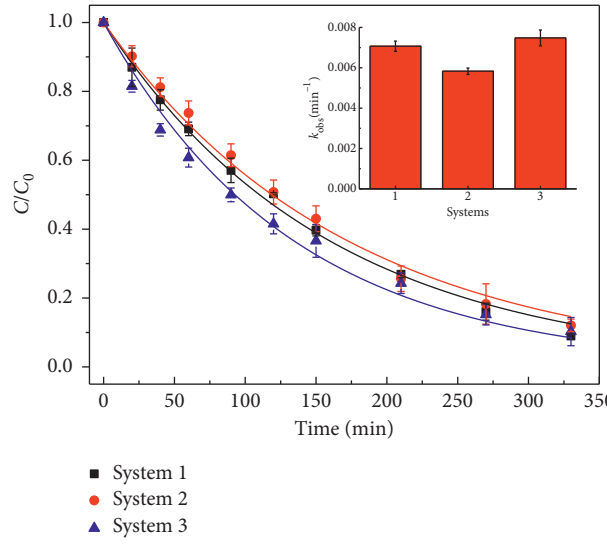

Figure 9: Effects of dissolved oxygen on AMO degradation by TAP. Solid lines represent the pseudo-first-order kinetic model fits. Insert: changes of k_{obs} at different conditions. Experimental conditions: $[AMO]_0 = 0.1$ mM; $[PS]_0 = 10$ mM; $T = 50^\circ$C; reaction time = 330 min.

effect of dissolved oxygen on AMO degradation efficiency by TAP could be neglected. Therefore, AMO degradation by TAP could be carried out in both the oxic condition and anoxic condition.

3.5. Identification of Predominate Radical Species on AMO Degradation. Radical species on AMO degradation were tested and identified by EPR. As shown in Figure 10, the generation of DMPO-OH was obviously demonstrated by its

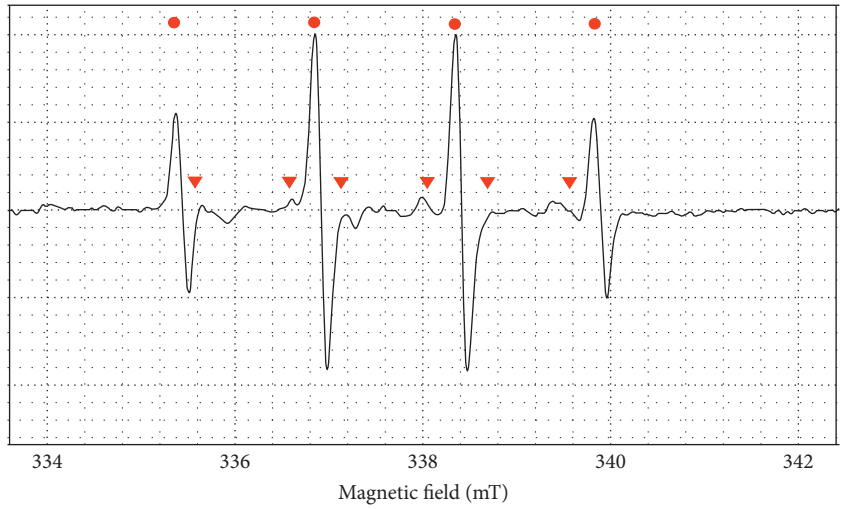

Figure 10: EPR spectrum of radical adducts in the TAP system. ● DMPO-OH, ▼ DMPO-SO_4. Experimental conditions: $[DMPO]_0 = 100$ mM; $[PS]_0 = 75$ mM; $T = 45^{\circ}C$; reaction time = 20 min.

hyperfine splitting constants ($A_N = A_H = 14.92$ G), suggesting that ·OH existed in the TAP system. DMPO-SO_4 was also monitored according to the simulation spectra ($A_N = 13.97$ G, $A_H = 9.94$ G, $A_H^{\gamma 1} = 1.44$ G, and $A_H^{\gamma 2} = 0.79$ G) [45]. Therefore, sulfate radical and hydroxyl radical were reactive oxidative species in the TAP system.

Furthermore, in order to identify the dominating reactive radicals on AMO degradation by TAP, MeOH (with α-hydrogen) and TBA (without α-hydrogen) were chosen as radical scavengers because of the different reaction constants between alcohol and radicals. The constant with which MeOH reacts with $SO_4^{\cdot-}$ (1.1×10^7 $M^{-1}{\cdot}s^{-1}$) is parallel to that with ·OH (9.7×10^8 $M^{-1}{\cdot}s^{-1}$), while the constant with which TBA reacts with $SO_4^{\cdot-}$ (4.0–9.1×10^5 $M^{-1}{\cdot}s^{-1}$) is much lower than that with ·OH (3.8–7.6×10^8 $M^{-1}{\cdot}s^{-1}$) [46]. Thus, MeOH is considered to scavenge both $SO_4^{\cdot-}$ and ·OH with a similar rate constant, and TBA is considered to scavenge ·OH efficiently. As depicted in Figure 11, after the addition of MeOH and TBA, the AMO degradation efficiency was observed to be approximately 53 and 59%, respectively, suggesting that $SO_4^{\cdot-}$ was the dominating radical in degrading AMO by TAP.

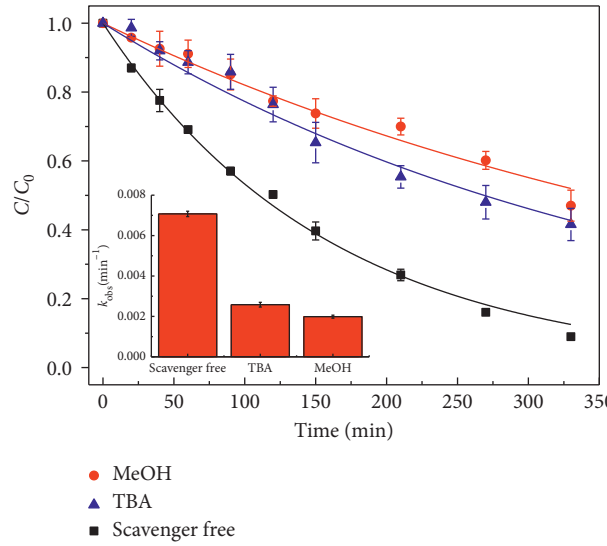

Figure 11: Effects of different scavengers on AMO degradation by TAP. Solid lines represent the pseudo-first-order kinetic model fits. Insert: changes of k_{obs} at different scavengers. Experimental conditions: $[AMO]_0 = 0.1$ mM; $[PS]_0 = 10$ mM; $T = 50^{\circ}C$, $[alcohol]_0/[PS]_0/[AMO]_0 = 30000:100:1$; reaction time = 330 min.

3.6. Performance of AMO Degradation by TAP in Real Waters. In order to evaluate the feasibility of applying TAP to degrade AMO under real environmental conditions, groundwater and drinking water were applied (Table 2). AMO degradation by TAP in groundwater and drinking water is shown in Figure 12. It could be seen that AMO degradation in groundwater and drinking water followed a pseudo-first-order kinetic model, and k_{obs} in groundwater was slightly higher than that in drinking water. This result was possibly because higher Cl^- concentration could promote AMO degradation efficiency according to the previous study (as shown in Section 3.4.1). Compared with deionized water, AMO degradation efficiency in groundwater and drinking water was a little lower probably due to the relatively high ionic strength which might hinder the degradation of contaminants in TAP, suggesting that application of TAP for remediation of AMO in groundwater and drinking water might be efficient.

4. Conclusions

In this study, AMO degradation by TAP was effectively achieved in aqueous solution. For any experiment condition, AMO degradation followed a pseudo-first-order kinetic model. The apparent activate energy of AMO degradation was calculated to be 126.9 $kJ{\cdot}mol^{-1}$ according to the Arrhenius equation ranged from 35°C to 60°C. On increasing

Table 2: Characteristics of water samples.

Waters	pH	Cl^-	NO_2^-	NO_3^-	SO_4^{2-}	$H_2PO_4^-$	Na^+	NH_4^+	K^+	Mg^{2+}	Ca^{2+}
Groundwater	7.61	39.7982	n.d.	0.0412	39.6060	n.d.	25.74	0.26	0.66	27.09	65.90
Drinking water	7.98	11.9522	n.d.	1.3448	14.2461	n.d.	71.29	n.d.	1.42	11.00	40.92

n.d., not detected.

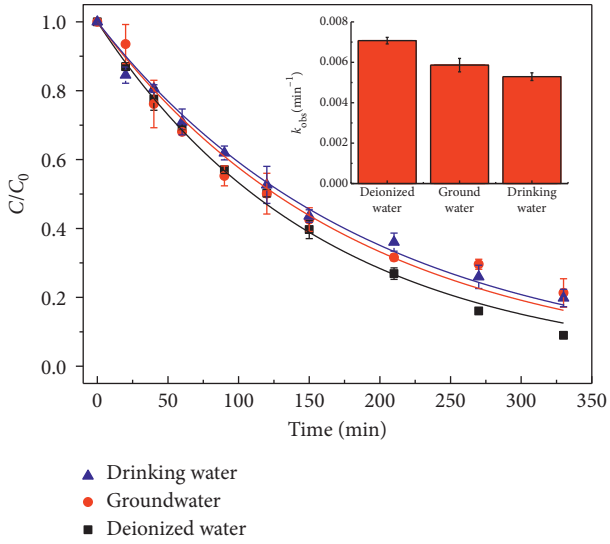

Figure 12: Effects of different real waters on AMO degradation by TAP. Solid lines represent the pseudo-first-order kinetic model fits. Insert: changes of k_{obs} at different real waters. Experimental conditions: $[AMO]_0 = 0.1$ mM; $[PS]_0 = 10$ mM; $T = 50^{\circ}C$; reaction time = 330 min.

the reaction temperature and the initial persulfate concentration, a decreasing pH significantly increased the AMO degradation efficiency. The EPR test demonstrated that both ·OH and $SO_4^{\cdot-}$ were generated in the TAP system, and the radical scavenging test identified that the predominant reactive radical species were $SO_4^{\cdot-}$ in aqueous solution without adjusting the solution pH. In groundwater and drinking water, AMO degradation suggested that TAP could be a reliable technology for water remediation contaminated by AMO in practice.

Data Availability

All of the data used to support the findings of this study are included within the article.

Conflicts of Interest

The authors declare that they have no conflicts of interest.

Acknowledgments

This study was supported by the National Natural Science Foundation of China (Grant nos. 51378064 and 51678054), Fundamental Research Funds for the Central Universities (Grant no. ZH1202B), and Science and Technology Planning Project of Langfang City (Grant no. 2017013150).

References

[1] Q. Gao, Y. Li, Z. Qi et al., "Diverse and abundant antibiotic resistance genes from mariculture sites of China's coastline," *Science of the Total Environment*, vol. 630, pp. 117–125, 2018.

[2] E. M. Eckert, A. D. Cesare, M. Coci, and G. Corno, "Persistence of antibiotic resistance genes in large subalpine lakes: the role of anthropogenic pollution and ecological interactions," *Hydrobiologia*, vol. 824, no. 1, pp. 93–108, 2018.

[3] W. Y. Mo, Z. Chen, H. M. Leung, and A. O. W. Leung, "Application of veterinary antibiotics in China's aquaculture industry and their potential human health risks," *Environmental Science and Pollution Research*, vol. 24, no. 10, pp. 8978–8989, 2017.

[4] R. Andreozzi, "Advanced oxidation processes (AOP) for water purification and recovery," *Catalysis Today*, vol. 53, no. 1, pp. 51–59, 1999.

[5] A. Ghauch, A. Baalbaki, M. Amasha, R. E. Asmar, and O. Tantawi, "Contribution of persulfate in UV-254 nm activated systems for complete degradation of chloramphenicol antibiotic in water," *Chemical Engineering Journal*, vol. 317, pp. 1012–1025, 2017.

[6] A. Ghauch, H. Baydoun, and P. Dermesropian, "Degradation of aqueous carbamazepine in ultrasonic/Fe^0/H_2O_2 systems," *Chemical Engineering Journal*, vol. 172, no. 1, pp. 18–27, 2011a.

[7] B.-T. Zhang, Y. Zhang, and Y. Teng, "Electrospun magnetic cobalt-carbon nanofiber composites with axis-sheath structure for efficient peroxymonosulfate activation," *Applied Surface Science*, vol. 452, pp. 443–450, 2018.

[8] A. Ghauch, A. M. Tuqan, N. Kibbi, and S. Geryes, "Methylene blue discoloration by heated persulfate in aqueous solution," *Chemical Engineering Journal*, vol. 213, pp. 259–271, 2012.

[9] A. Ghauch, A. M. Tuqan, and N. Kibbi, "Ibuprofen removal by heated persulfate in aqueous solution: a kinetics study," *Chemical Engineering Journal*, vol. 197, pp. 483–492, 2012.

[10] M. Amasha, A. Baalbaki, and A. Ghauch, "A comparative study of the common persulfate activation techniques for the complete degradation of an NSAID: the case of ketoprofen," *Chemical Engineering Journal*, vol. 350, pp. 395–410, 2018.

[11] S. Su, W. Guo, C. Yi, Y. Leng, and Z. Ma, "Degradation of amoxicillin in aqueous solution using sulphate radicals under ultrasound irradiation," *Ultrasonics Sonochemistry*, vol. 19, no. 3, pp. 469–474, 2012.

[12] J. Paul, D. B. Naik, Y. K. Bhardwaj, and L. Varshney, "Studies on oxidative radiolysis of ibuprofen in presence of potassium persulfate," *Radiation Physics and Chemistry*, vol. 100, pp. 38–44, 2014.

[13] G. Ayoub and A. Ghauch, "Assessment of bimetallic and trimetallic iron-based systems for persulfate activation: application to sulfamethoxazole degradation," *Chemical Engineering Journal*, vol. 256, pp. 280–292, 2014.

[14] A. Ghauch, G. Ayoub, and S. Naim, "Degradation of sulfamethoxazole by persulfate assisted micrometric Fe^0 in aqueous solution," *Chemical Engineering Journal*, vol. 228, pp. 1168–1181, 2013.

[15] S. Naim and A. Ghauch, "Ranitidine abatement in chemically activated persulfate systems: assessment of industrial iron waste for sustainable applications," *Chemical Engineering Journal*, vol. 288, pp. 276–288, 2016.

[16] B.-T. Zhang, Y. Zhang, Y. Teng, and M. Fan, "Sulfate radical and its application in decontamination technologies," *Critical Reviews in Environmental Science and Technology*, vol. 45, no. 16, pp. 1756–1800, 2015.

[17] A. Ghauch and A. Tuqan, "Oxidation of bisoprolol in heated persulfate/H_2O systems: kinetics and products," *Chemical Engineering Journal*, vol. 183, pp. 162–171, 2012.

[18] A. Ghauch, H. Baydoun, A. M. Tuqan, G. Ayoub, and S. Naim, "Submicrometric iron particles for the removal of pharmaceuticals from water: application to b-lactam antibiotics," *Advanced Materials Research*, vol. 324, pp. 485–488, 2011.

[19] A. Ghauch, A. Tuqan, and H. A. Assi, "Antibiotic removal from water: elimination of amoxicillin and ampicillin by microscale and nanoscale iron particles," *Environmental Pollution*, vol. 157, no. 5, pp. 1626–1635, 2009.

[20] F. Ay and F. Kargi, "Advanced oxidation of amoxicillin by Fenton's reagent treatment," *Journal of Hazardous Materials*, vol. 179, no. 1–3, pp. 622–627, 2010.

[21] V. Homem, A. Alves, and L. Santos, "Amoxicillin degradation at ppb levels by Fenton's oxidation using design of experiments," *Science of the Total Environment*, vol. 408, no. 24, pp. 6272–6280, 2010.

[22] O. B. Ayodele, J. K. Lim, and B. H. Hameed, "Pillared montmorillonite supported ferric oxalate as heterogeneous photo-Fenton catalyst for degradation of amoxicillin," *Applied Catalysis A: General*, vol. 413-414, pp. 301–309, 2012.

[23] A. G. Trovó, R. F. P. Nogueira, A. Agüera, A. R. F. Alba, and S. Malato, "Degradation of the antibiotic amoxicillin by photo-Fenton process–chemical and toxicological assessment," *Water Research*, vol. 45, no. 3, pp. 1394–1402, 2011.

[24] Y. J. Jung, W. G. Kim, Y. Yoon et al., "Removal of amoxicillin by UV and UV/H_2O_2 processes," *Science of the Total Environment*, vol. 420, pp. 160–167, 2012.

[25] V. Homem, A. Alves, and L. Santos, "Microwave-assisted fenton's oxidation of amoxicillin," *Chemical Engineering Journal*, vol. 220, pp. 35–44, 2013.

[26] D. Kanakaraju, J. Kockler, C. A. Motti, B. D. Glass, and M. Oelgemöller, "Titanium dioxide/zeolite integrated photocatalytic adsorbents for the degradation of amoxicillin," *Applied Catalysis B: Environmental*, vol. 166-167, pp. 45–55, 2015.

[27] N. F. Moreira, C. A. Orge, A. R. Ribeiro et al., "Fast mineralization and detoxification of amoxicillin and diclofenac by photocatalytic ozonation and application to an urban wastewater," *Water Research*, vol. 87, pp. 87–96, 2015.

[28] M. Benacherine, N. Debbache, I. Ghoul, and Y. Mameri, "Heterogeneous photoinduced degradation of amoxicillin by goethite under artificial and natural irradiation," *Journal of Photochemistry and Photobiology A: Chemistry*, vol. 335, pp. 70–77, 2017.

[29] C. Liang, C.-F. Huang, N. Mohanty, and R. M. Kurakalva, "A rapid spectrophotometric determination of persulfate anion in ISCO," *Chemosphere*, vol. 73, no. 9, pp. 1540–1543, 2008.

[30] H. P. Gao, C.-F. Huang, N. Mohanty, and R. M. Kurakalva, "Sulfate radicals induced degradation of Triclosan in thermally activated persulfate system," *Chemical Engineering Journal*, vol. 306, pp. 522–530, 2016.

[31] A. Ghauch, A. Tuqan, and N. Kibbi, "Naproxen abatement by thermally activated persulfate in aqueous systems," *Chemical Engineering Journal*, vol. 279, pp. 861–873, 2015.

[32] C. Q. Tan, N. Gao, Y. Deng, N. An, and J. Deng, "Heat-activated persulfate oxidation of diuron in water," *Chemical Engineering Journal*, vol. 203, pp. 294–300, 2012.

[33] J. F. Yang, L.-M. Yang, S.-B. Zhang et al., "Degradation of azole fungicide fluconazole in aqueous solution by thermally activated persulfate," *Chemical Engineering Journal*, vol. 321, pp. 113–122, 2017.

[34] J. Chen, Y. Qian, H. Liu, and T. Huang, "Oxidative degradation of diclofenac by thermally activated persulfate: implication for ISCO," *Environmental Science and Pollution Research*, vol. 23, no. 4, pp. 3824–3833, 2016.

[35] M. H. Nie, Y. Yang, and Z. Zhang, "Degradation of chloramphenicol by thermally activated persulfate in aqueous solution," *Chemical Engineering Journal*, vol. 246, pp. 373–382, 2014.

[36] C. Jiang, Y. Ji, Y. Shi, J. Chen, and T. Cai, "Sulfate radical-based oxidation of fluoroquinolone antibiotics: kinetics, mechanisms and effects of natural water matrices," *Water Research*, vol. 106, pp. 507–517, 2016.

[37] P. Neta, V. Madhavan, H. Zemel, and R. W. Fessenden, "Rate constants and mechanism of reaction of $SO_4^{\cdot-}$ with aromatic compounds," *Journal of the American Chemical Society*, vol. 99, no. 1, pp. 163-164, 1977.

[38] G. Huang, C. T. Aravindakumar, and B. S. M. Rao, "Pulse radiolysis study of the reactions of $SO_4^{\cdot-}$ with some substituted benzenes in aqueous solution," *Journal of the Chemical Society, Faraday Transactions*, vol. 90, no. 4, pp. 597–604, 1994.

[39] J. J. Pignatello, E. Oliveros, and A. MacKay, "Advanced oxidation processes for organic contaminant destruction based on the fenton reaction and related chemistry," *Critical Reviews in Environmental Science and Technology*, vol. 36, no. 1, pp. 1–84, 2006.

[40] Y. Fan, Y. Ji, D. Kong, J. Lu, and Q. Zhou, "Kinetic and mechanistic investigations of the degradation of sulfamethazine in heat-activated persulfate oxidation process," *Journal of Hazardous Materials*, vol. 300, pp. 39–47, 2015.

[41] G. V. Buxton, M. Bydder, and G. A. Salmon, "The reactivity of chlorine atoms in aqueous solution part II. The equilibrium $SO_4^{\cdot-}+Cl^- = Cl^{\cdot}+SO_4^{2-}$," *Physical Chemistry Chemical Physics*, vol. 1, no. 2, pp. 269–273, 1999.

[42] Y. Feng, Q. Song, W. Song, and G. Liu, "Degradation of ketoprofen by sulfate radical-based advanced oxidation processes: kinetics, mechanisms, and effects of natural water matrices," *Chemosphere*, vol. 189, pp. 643–651, 2017.

[43] G. Fang, J. Gao, D. D. Dionysiou, C. Liu, and D. Zhou, "Activation of persulfate by quinones: free radical reactions and implication for the degradation of PCBs," *Environmental Science & Technology*, vol. 47, no. 9, pp. 4605–4611, 2013.

[44] M. Ahmad, A. L. Teel, and R. J. Watts, "Mechanism of persulfate activation by phenols," *Environmental Science & Technology*, vol. 47, no. 11, pp. 5864–5871, 2013.

[45] O. S. Furman, A. L. Teel, and R. J. Watts, "Mechanism of base activation of persulfate," *Environmental Science & Technology*, vol. 44, no. 16, pp. 6423–6428, 2010.

[46] C. L. Qian and R. E. Huie, "Rate constants for hydrogen abstraction reactions of the sulfate radical, $SO_4^{\cdot-}$ Alcohols," *International Journal of Chemical Kinetics*, vol. 21, no. 8, pp. 677–687, 1989.